

## Field-induced condensation of magnons and long range order in $\text{BaCuSi}_2\text{O}_6$

This article has been downloaded from IOPscience. Please scroll down to see the full text article.

2006 J. Phys.: Condens. Matter 18 4719

(<http://iopscience.iop.org/0953-8984/18/19/023>)

View [the table of contents for this issue](#), or go to the [journal homepage](#) for more

Download details:

IP Address: 129.252.86.83

The article was downloaded on 28/05/2010 at 10:42

Please note that [terms and conditions apply](#).

# Field-induced condensation of magnons and long range order in $\text{BaCuSi}_2\text{O}_6$

Han-Ting Wang, Bao Xu and Yupeng Wang

Beijing National Laboratory of Condensed Matter Physics and Institute of Physics, Chinese Academy of Sciences, Beijing 100080, People's Republic of China

Received 6 February 2006, in final form 21 March 2006

Published 27 April 2006

Online at [stacks.iop.org/JPhysCM/18/4719](http://stacks.iop.org/JPhysCM/18/4719)

## Abstract

A quasi-two-dimensional antiferromagnet with a square-lattice bilayer structure is studied with a bond operator formalism. The excitation spectrum and its temperature dependence, the quantum phase transition from the spin-singlet dimerized state to the Néel state, are studied. In particular the field-induced long range order is interpreted using Bose–Einstein condensation of magnons. The phase diagram as well as the temperature and magnetic field dependences of the specific heat and the staggered magnetization are studied. The critical exponents around the critical magnetic fields  $H_{c1}$  and  $H_{c2}$  are calculated to be about 1.5. These results agree well with recent experimental results for  $\text{BaCuSi}_2\text{O}_6$ .

## 1. Introduction

Quantum low-dimensional antiferromagnets have attracted a great deal of attention in the past decades. A Heisenberg antiferromagnet on a double-layer square lattice was used by Millis and Monien [1] as a phenomenological model to capture the spin-gap behaviour observed in high- $T_c$  compounds such as  $\text{YBa}_2\text{Cu}_3\text{O}_{6+x}$  and  $\text{Bi}_2\text{Sr}_2\text{CaCu}_2\text{O}_8$ . Quantum Hall systems, especially, bilayer quantum Hall systems at a filling factor  $\nu = 2$  [2, 3], which can be well described by a Heisenberg model, have provided another platform for studying the zero temperature quantum transitions between states with different spin magnetizations. Recently, the material  $\text{BaCuSi}_2\text{O}_6$ , containing strongly coupled bilayers, has been discovered and investigated [4–6] in detail. It shows a spin gap, and the gap increases with increasing temperature [4]. When a strong enough external magnetic field is applied, the energy gap closes and a phase transition is observed for the measurements of specific heat, the magnetocaloric effect (MCE) and magnetization [5]. These results are well explained by a Monte Carlo simulation on a reduced effective hard-core boson model [5]. A critical exponent of  $\nu = 0.63 \pm 0.03$  is obtained around the critical magnetic field  $H_{c1} = 23.52$  T [6], which is in good agreement with the mean field prediction of  $\nu = \frac{2}{3}$  for the three-dimensional XY model. Field-induced long range order in the plane perpendicular to the external magnetic field was observed in other similar systems

such as  $S = 1$  antiferromagnetic chains [7], antiferromagnetic spin dimers [8], even-leg spin ladders [9],  $S = \frac{1}{2}$  alternating chains or frustrated spin systems [10] and an  $S = 1$  three-dimensional antiferromagnet with large single-ion anisotropy [11]. These experiments are interpreted with the idea of Bose–Einstein condensation (BEC) of magnons [12, 13], and some of them have been studied theoretically with quantum Monte Carlo simulations [14, 15], Bose–Einstein Hartree–Fock theory [16, 17] and bond operator mean field theory [18, 19]. Although the experimentally reported critical exponent  $\alpha$  is discrete to some extent, the theoretical result converges to 1.5.

Concerned with the material BaCuSi<sub>2</sub>O<sub>6</sub>, we study a coupled bilayer system described by the Hamiltonian

$$H = J \sum_{\vec{r}} \vec{S}_{\vec{r}1} \cdot \vec{S}_{\vec{r}2} + \frac{1}{2} J' \sum_{\vec{r}, \delta_1} (\vec{S}_{\vec{r}1} \cdot \vec{S}_{\vec{r}+\delta_1 1} + \vec{S}_{\vec{r}2} \cdot \vec{S}_{\vec{r}+\delta_1 2}) + \frac{1}{2} J'' \sum_{\vec{r}} (\vec{S}_{\vec{r}1} \cdot \vec{S}_{\vec{r}+\vec{e}_z 2} + \vec{S}_{\vec{r}2} \cdot \vec{S}_{\vec{r}-\vec{e}_z 1}) - g \mu_B B \sum_{\vec{r}} (S_{\vec{r}1}^z + S_{\vec{r}2}^z), \quad (1)$$

where  $\sum_{\vec{r}}$  sums over the singlet bonds and  $\vec{\delta}_1 = \pm \vec{e}_x, \pm \vec{e}_y$  denotes the nearest neighbours in the  $x$ - $y$  plane. An external magnetic field is applied with  $\mu_B$  the Bohr magneton. When  $J'' = 0$ , the model (1) reduces to an isolated two-layer system and has been studied extensively. At a critical  $(\frac{J'}{J})_c \sim 0.4$ , a transition from a disordered gapped state to Néel state occurs [20–22]. The field- and temperature-dependent properties, such as susceptibility and specific heat, are studied with the strong coupling expansions [23–25]. Although the ground state phase diagram in the external magnetic field and the transition features have been studied [26, 27], the phase transitions at finite temperatures are less studied. In this paper we use the bond operator formalism to study the model (1). In particular we will study the phase transition induced by the Bose–Einstein condensation of magnons. In section 2 we give the self-consistent equations based on the bond operator formalism. In section 3 we study the effects of  $J''$  on the quantum phase transitions. Including  $J''$  will decrease the critical value  $J'_c$ . In section 4, we study the phase transitions induced by applying an external magnetic field. Corresponding to a given magnetic field, a critical temperature  $T_c(h)$  exists below which the Bose–Einstein condensation of magnons occurs and long range order in the plane perpendicular to the external magnetic field is induced. The phase diagram at finite temperature is given. The critical exponents around  $H_{c1}$  and  $H_{c2}$  are calculated to be about 1.5. The dependences of specific heat and the staggered magnetization on temperature and magnetic field are also studied. These results agree well with the experimental results for BaCuSi<sub>2</sub>O<sub>6</sub>. The dimensional crossover behaviour with  $J''$  approaching 0 is also discussed. A summary is given in section 5.

## 2. Self-consistent equations based on the bond operator formalism

For two  $S = \frac{1}{2}$  spins there are four eigenstates and four boson operators were introduced [28]:

$$\begin{aligned} |00\rangle &= s^\dagger |v\rangle = \frac{1}{\sqrt{2}} (|\uparrow\downarrow\rangle - |\downarrow\uparrow\rangle) \\ |11\rangle &= u^\dagger |v\rangle = |\uparrow\uparrow\rangle, \\ |10\rangle &= t_z^\dagger |v\rangle = \frac{1}{\sqrt{2}} (|\uparrow\downarrow\rangle + |\downarrow\uparrow\rangle), \\ |1-1\rangle &= d^\dagger |v\rangle = |\downarrow\downarrow\rangle, \end{aligned} \quad (2)$$

where  $|v\rangle$  is the vacuum state and we use the eigenstates of  $|11\rangle$  and  $|1-1\rangle$  to study the effects of a magnetic field [29]. With a constraint  $s^\dagger s + u^\dagger u + d^\dagger d + t_z^\dagger t_z = 1$ , the spin operators can

be represented by

$$\begin{aligned} S_{1,2}^+ &= \frac{1}{\sqrt{2}}(\pm s^\dagger d \mp u^\dagger s + t_z^\dagger d + u^\dagger t_z), \\ S_{1,2}^- &= (S_{1,2}^+)^\dagger, \\ S_{1,2}^z &= \frac{1}{2}(\pm s^\dagger t_z \pm t_z^\dagger s + u^\dagger u - d^\dagger d). \end{aligned} \quad (3)$$

Substituting the above boson representation into the original Hamiltonian (1) and assuming the  $s$  bosons are condensed,  $\langle s \rangle = \langle s^\dagger \rangle = s$ , we get

$$H = H(J) + H(J') + H(J'') + H(h) + H(\mu) \quad (4)$$

with

$$\begin{aligned} H(J) &= -\frac{3}{4}JNs^2 + \frac{1}{4}J \sum_{\vec{r}} (u_{\vec{r}}^\dagger u_{\vec{r}} + t_{z\vec{r}}^\dagger t_{z\vec{r}} + d_{\vec{r}}^\dagger d_{\vec{r}}) \\ H(J') &= \frac{1}{4}J' \sum_{\vec{r}, \delta_1} [s^2 (d_{\vec{r}} - u_{\vec{r}}^\dagger) (d_{\vec{r}+\delta_1}^\dagger - u_{\vec{r}+\delta_1}^\dagger) + (t_{z\vec{r}}^\dagger d_{\vec{r}} + u_{\vec{r}}^\dagger t_{z\vec{r}}) (t_{z\vec{r}+\delta_1}^\dagger d_{\vec{r}+\delta_1}^\dagger + u_{\vec{r}+\delta_1}^\dagger t_{z\vec{r}+\delta_1}^\dagger) \\ &\quad + \text{h.c.} + s^2 (t_{z\vec{r}} + t_{z\vec{r}}^\dagger) (t_{z\vec{r}+\delta_1} + t_{z\vec{r}+\delta_1}^\dagger) \\ &\quad + (u_{\vec{r}}^\dagger u_{\vec{r}} - d_{\vec{r}}^\dagger d_{\vec{r}}) (u_{\vec{r}+\delta_1}^\dagger u_{\vec{r}+\delta_1} - d_{\vec{r}+\delta_1}^\dagger d_{\vec{r}+\delta_1})] \\ H(J'') &= \frac{1}{8}J'' \sum_{\vec{r}, \delta_2} [s^2 (d_{\vec{r}} - u_{\vec{r}}^\dagger) (-d_{\vec{r}+\delta_2}^\dagger + u_{\vec{r}+\delta_2}^\dagger) + (t_{z\vec{r}}^\dagger d_{\vec{r}} + u_{\vec{r}}^\dagger t_{z\vec{r}}) (t_{z\vec{r}+\delta_2}^\dagger d_{\vec{r}+\delta_2}^\dagger \\ &\quad + u_{\vec{r}+\delta_2}^\dagger t_{z\vec{r}+\delta_2}^\dagger) + \text{h.c.} - s^2 (t_{z\vec{r}} + t_{z\vec{r}}^\dagger) (t_{z\vec{r}+\delta_2} + t_{z\vec{r}+\delta_2}^\dagger) \\ &\quad + (u_{\vec{r}}^\dagger u_{\vec{r}} - d_{\vec{r}}^\dagger d_{\vec{r}}) (u_{\vec{r}+\delta_2}^\dagger u_{\vec{r}+\delta_2} - d_{\vec{r}+\delta_2}^\dagger d_{\vec{r}+\delta_2})] \\ H(h) &= -h \sum_{\vec{r}} (u_{\vec{r}}^\dagger u_{\vec{r}} - d_{\vec{r}}^\dagger d_{\vec{r}}) \\ H(\mu) &= - \sum_{\vec{r}} \mu_{\vec{r}} (s^2 + u_{\vec{r}}^\dagger u_{\vec{r}} + t_{z\vec{r}}^\dagger t_{z\vec{r}} + d_{\vec{r}}^\dagger d_{\vec{r}} - 1) \end{aligned} \quad (5)$$

where  $\delta_2 = \pm \vec{e}_z$ ,  $h = g\mu_B B$  and a temperature-dependent chemical potential  $\mu_{\vec{r}}$  is introduced to impose the constraint condition of single occupancy. As shown by Kotov *et al* with the Brueckner approach [22], the density of the triplet excitations is a small parameter and all anomalous contributions are suppressed. The contribution from the four-operator terms is small. By a mean-field approximation, we replace the local constraint by a global one and let  $\mu_{\vec{r}} = \mu$  [28]. When  $s^2$  is close to 1 or the density of the excitations is small, this mean-field approximation is proved to be quite effective. Another approach to deal with the single occupancy condition was developed by Popov and Fedotov [30]. In their functional integral formalism they use a fermion representation and introduce a purely imaginative chemical potential  $\mu = \frac{i\pi}{2\beta}$  for  $S = \frac{1}{2}$  spins and  $\mu = \frac{i\pi}{3\beta}$  for  $S = 1$  spins to eliminate the nonphysical states. The technique was then generalized for arbitrary spins [31] with a set of imaginary chemical potentials  $\mu_l = \frac{i\pi}{\beta} \frac{2l+1}{2s+1}$ .  $J$  is set to 1 in the following calculations. We make mean-field decoupling to the four-operator term<sup>1</sup>

$$(u_{\vec{r}}^\dagger u_{\vec{r}} - d_{\vec{r}}^\dagger d_{\vec{r}}) (u_{\vec{r}+\delta}^\dagger u_{\vec{r}+\delta} - d_{\vec{r}+\delta}^\dagger d_{\vec{r}+\delta}) = 2m(u_{\vec{r}}^\dagger u_{\vec{r}} - d_{\vec{r}}^\dagger d_{\vec{r}}) - m^2 \quad (6)$$

with  $m = \langle u_{\vec{r}}^\dagger u_{\vec{r}} \rangle - \langle d_{\vec{r}}^\dagger d_{\vec{r}} \rangle$ . After a Fourier–Bogoliubov transformation, we get the diagonalized Hamiltonian

$$H = \sum_k (\omega_k^{(1)} \alpha_k^\dagger \alpha_k + \omega_k^{(2)} \beta_k^\dagger \beta_k + \Omega_k \eta_k^\dagger \eta_k) + \sum_k \frac{1}{2} (2\omega_k + \Omega_k - A_k - B_k - D_k) + c, \quad (7)$$

<sup>1</sup> The three-operator terms such as  $(d_{\vec{r}} - u_{\vec{r}}^\dagger) (t_{z\vec{r}+\delta_1}^\dagger d_{\vec{r}+\delta_1}^\dagger + u_{\vec{r}+\delta_1}^\dagger t_{z\vec{r}+\delta_1}^\dagger)$  are omitted. The other four-operator terms can be considered by introducing the mean-field amounts  $p_d = \langle d_{\vec{r}+\delta_1}^\dagger d_{\vec{r}} \rangle$ ,  $p_u = \langle u_{\vec{r}+\delta_1}^\dagger u_{\vec{r}} \rangle$ ,  $p_t = \langle t_{\vec{r}+\delta_1}^\dagger t_{\vec{r}} \rangle$ ,  $p'_d = \langle d_{\vec{r}+\delta_2}^\dagger d_{\vec{r}} \rangle$ ,  $p'_u = \langle u_{\vec{r}+\delta_2}^\dagger u_{\vec{r}} \rangle$ ,  $p'_t = \langle t_{\vec{r}+\delta_2}^\dagger t_{\vec{r}} \rangle$ ,  $q_1 = \langle u_{\vec{r}+\delta_1}^\dagger d_{\vec{r}} \rangle$ ,  $q_2 = \langle t_{\vec{r}+\delta_1}^\dagger t_{\vec{r}} \rangle$ ,  $q'_1 = \langle u_{\vec{r}+\delta_2}^\dagger d_{\vec{r}} \rangle$  and  $q'_2 = \langle t_{\vec{r}+\delta_2}^\dagger t_{\vec{r}} \rangle$ . These terms have little effect on the numerical results.

where  $\alpha_k = \chi_k u_k + \rho_k d_{-k}^\dagger$ ,  $\beta_k = \chi_k d_{-k} + \rho_k u_k^\dagger$  with  $\chi_k^2 = \frac{1}{2}(1 + \frac{A_k+B_k}{2\omega_k})$  and  $\rho_k^2 = \frac{1}{2}(-1 + \frac{A_k+B_k}{2\omega_k})$ ;  $\eta_k = \theta_k t_k + \phi_k t_{-k}^\dagger$  with  $\theta_k^2 = \frac{1}{2}(1 + \frac{D_k}{\Omega_k})$  and  $\phi_k^2 = \frac{1}{2}(-1 + \frac{D_k}{\Omega_k})$ . The energy gap  $\Delta_0$  occurs at  $\vec{k}_0 = (\pi, \pi, 0)$ . The ground state energy per bond is  $e_0 = \frac{1}{2N} \sum_k (2\omega_k + \Omega_k - A_k - B_k - D_k) + \frac{1}{N}c$ . The Gibbs free energy  $G = Ne_0 - \frac{1}{\beta} \sum_k \ln[1 + n(\omega_k^{(1)})] - \frac{1}{\beta} \sum_k \ln[1 + n(\omega_k^{(2)})] - \frac{1}{\beta} \sum_k \ln[1 + n(\Omega_k)]$  with  $n(\omega_k) = \frac{1}{e^{\beta\omega_k} - 1}$  and  $\beta = \frac{1}{k_B T}$ . For brevity, we present the self-consistent equations for  $s^2$ ,  $\mu$  and  $m$  in appendix A.

### 3. Quantum phase transitions induced by changing $J'$ and $J''$

We first study the case of  $h = 0$ . Without an external magnetic field, the magnetization  $m$  is zero. At zero temperature, the self-consistent equations can be simplified as:

$$\begin{aligned} s^2 &= \frac{5}{2} - \frac{3}{4}[I_1(d_1, d_2) + I_2(d_1, d_2)], \\ \mu &= -\frac{3}{4} + \frac{3}{4s^2} \left( \frac{1}{4} - \mu \right) [I_2(d_1, d_2) - I_1(d_1, d_2)] \end{aligned} \quad (8)$$

with

$$\begin{aligned} d_1 &= \frac{4J's^2}{\frac{1}{4} - \mu}, \\ d_2 &= \frac{J''s^2}{\frac{1}{4} - \mu}, \\ I_1(d_1, d_2) &= \frac{1}{N} \sum_k \frac{1}{\sqrt{1 + d_1\gamma_k - d_2\gamma'_k}}, \\ I_2(d_1, d_2) &= \frac{1}{N} \sum_k \sqrt{1 + d_1\gamma_k - d_2\gamma'_k}. \end{aligned} \quad (9)$$

A single equation about  $d_1$  can then be obtained

$$1 - \frac{10J'}{d_1} + \frac{6J'}{d_1} I_1\left(d_1, \frac{J''}{4J'} d_1\right) = 0. \quad (10)$$

The excitation spectrum is  $\omega_k = \Omega_k = (\frac{1}{4} - \mu)\sqrt{1 + d_1\gamma_k - d_2\gamma'_k}$ . According to the experiments on BaCuSi<sub>2</sub>O<sub>6</sub>, we choose  $J' = 0.13J$  and  $J'' = 0.026J$  [4, 5]. Solving the self-consistent equations at  $T = 0$  numerically, we get  $s^2 = 0.9864$ ,  $\mu = -0.7770$  and the energy gap  $\Delta_0 = \omega_{\vec{k}_0} = 0.7082J = 3.15$  meV with  $J = 4.45$  meV, which agrees well with the experimental value 3.13 meV. (With the revised parameters [6].  $J' = 0.51$  meV = 0.1146 $J$ ,  $J'' = 0.168$  meV = 0.03775 $J$ , the numerical results are  $s^2 = 0.9848$ ,  $\mu = -0.7709$ , and  $\Delta = 0.7355J$ .) The temperature dependence of the energy gap is also studied by solving equation (15). In figure 1, we show the change of the energy gap with increasing temperature. The energy gap changes little at low temperatures and increases fast at larger temperatures<sup>2</sup>. We do not get a trend to a plateau value, as observed in the experiment [4]. The reason for this may be that the value of  $s^2$  is small at higher temperatures and the approximation of  $\langle s^\dagger \rangle = \langle s \rangle = s$  becomes less good.

<sup>2</sup> When  $p_u, p_d, p_t, p'_u, p'_d, p'_t, q_1, q_2, q'_1$  and  $q'_2$  are included, the degeneracy between  $\omega_k$  and  $\Omega_k$  will be lifted and the longitudinal fluctuation  $\eta_k$  becomes a little lower. The energy gap also occurs at  $\vec{k}_0 = (\pi, \pi, 0)$  with  $\Delta_0 = \Omega_{\vec{k}_0} = 0.7410J$  and  $\omega_{\vec{k}_0} = 0.7436J$ . The correction is very small.

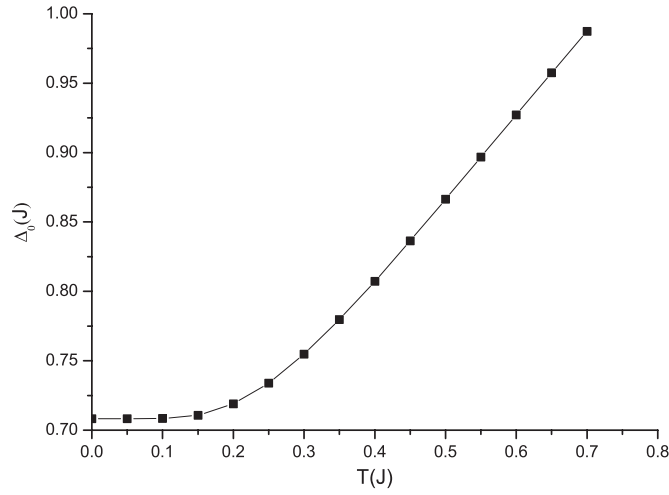


**Figure 1.** The energy gap increases with increasing temperature. The parameters are  $J' = 0.13J$  and  $J'' = 0.026J$ .

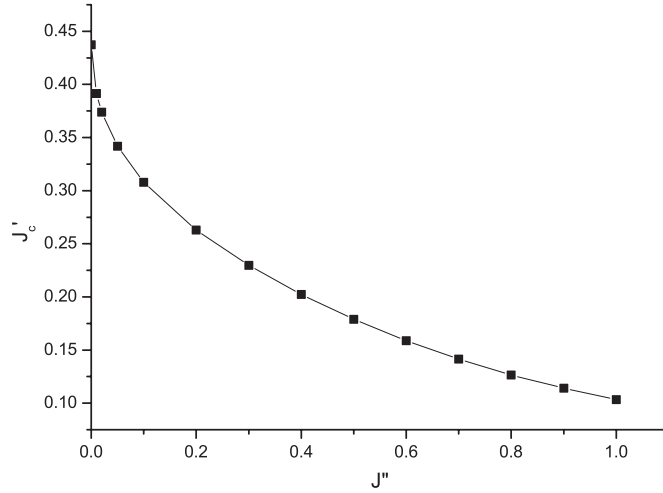


**Figure 2.** The critical  $J'_c$  decreases with increasing  $J''$ .

When  $d_1 + d_2 = 1$ , the energy gap goes to 0, which indicates a transition from the disordered phase to the Néel phase. The critical  $J'$  and  $J''$  can be obtained from the equation

$$\begin{aligned}
 J' &= \frac{1}{\frac{10}{d_1} - \frac{6}{d_1} I_1(d_1, 1 - d_1)} \\
 J'' &= 4J' \frac{1 - d_1}{d_1}.
 \end{aligned}
 \tag{11}$$

For a given  $d_1$ , we calculate  $J'$  and  $J''$ , respectively. At  $J'' = 0$ , the corresponding  $J' = 0.432$ , in agreement with the numerical results and other analytical results [20–22]. In figure 2, we show the critical  $J''$ – $J'_c$  curve. The critical  $J'_c$  decreases with increasing  $J''$ .

#### 4. Field-induced long range order and condensation of magnons

When an external magnetic field is applied, the excitation spectrum splits into three branches as expressed in appendix A. In particular, the branch  $\omega_k^{(1)}$  decreases with increasing magnetic field and the energy gap goes to zero at a critical magnetic field  $h_{c1} = \Delta_0 = \omega_k|_{k=(\pi,\pi,0)}$ . When  $h > h_{c1}$ , we assume that the energy gap stays at zero and the corresponding excitations condense [19, 32]. A BEC amounting to  $n_h(T) = \frac{1}{N} \langle \alpha_k^\dagger \alpha_k \rangle_{\frac{A_k+B_k}{2\omega_k}}|_{k=(\pi,\pi,0)}$  can then be extracted and the self-consistent equations become

$$\begin{aligned} s^2 &= \frac{5}{2} - n_h(T) - \frac{1}{N} \sum_k \frac{A_k + B_k}{2\omega_k} [n(\omega_k^{(1)}) + n(\omega_k^{(2)}) + 1] - \frac{1}{N} \sum_k \frac{D_k}{\Omega_k} \left[ n(\Omega_k) + \frac{1}{2} \right], \\ \mu &= -\frac{3}{4} - \left( \frac{1}{2} + \frac{C_{(\pi,\pi,0)}}{A_{(\pi,\pi,0)} + B_{(\pi,\pi,0)}} \right) \left( zJ' + \frac{1}{2}z'J'' \right) n_h(T) \\ &\quad + \frac{1}{N} \sum_k \left[ \frac{A_k + B_k + 2C_k}{4\omega_k} [1 + n(\omega_k^{(1)}) + n(\omega_k^{(2)})] \right. \\ &\quad \left. + \left[ n(\Omega_k) + \frac{1}{2} \right] \frac{D_k - 2F_k}{2\Omega_k} \right] \left( zJ'\gamma_k - \frac{1}{2}z'J''\gamma'_k \right), \\ m &= \frac{2\omega_{(\pi,\pi,0)}}{A_{(\pi,\pi,0)} + B_{(\pi,\pi,0)}} n_h(T) + \frac{1}{N} \sum_k [n(\omega_k^{(1)}) - n(\omega_k^{(2)})], \end{aligned} \quad (12)$$

where the summation  $\sum_k \dots n(\omega_k^{(1)})$  does not include  $\vec{k}_0 = (\pi, \pi, 0)$ . A condition

$$\omega_{\vec{k}_0} - h + \left( \frac{1}{2}zJ' + \frac{1}{4}z'J'' \right) m = 0, \quad (13)$$

should be added to maintain the energy gap at zero.

A field-induced staggered magnetization in the plane perpendicular to the magnetic field has been observed in many systems [5–11], and can be explained by the condensation of magnons. The staggered magnetization can be obtained by calculating the spin–spin correlation function [32] or by calculating the average  $\langle S_{\vec{r}}^x \rangle$  directly<sup>3</sup>:

$$m_x = s \sqrt{\frac{n_h(T)}{2 - d_1 - d_2}}, \quad (14)$$

where  $d_1$  and  $d_2$  are defined in equation (9).

Equations (12)–(14) tell us that a uniform magnetization  $m$  parallel to the external magnetic field and a staggered magnetization  $m_x$  in the plane perpendicular to the applied field will appear with the  $\alpha_k$  bosons condensed at  $\vec{k}_0$ . However, at a second critical magnetic field  $h_{c2}$ , where the magnetization saturates (i.e. all the dimers are in the state of  $u^\dagger|v\rangle$  and hence  $s = 0$ ), the staggered magnetization will disappear. For a given magnetic field  $h_{c1} < h < h_{c2}$ , the BEC density  $n_h(T)$  decreases with increasing temperature and goes to zero at a certain temperature, which defines the critical temperature  $T_c(h)$ . In the following, we present the numerical results.

In the numerical solutions, we still insert the parameters of BaCuSi<sub>2</sub>O<sub>6</sub> ( $J = 4.45$  meV,  $J' = 0.13J$  and  $J'' = 0.026J$ ), and compare our results with the experimental data. Figure 3(a) (solid line with squares) exhibits the critical temperature  $T_c(H)$  as a function

<sup>3</sup> The staggered magnetization can also be calculated as follows. From equation (3), we have  $S_{1\vec{r}}^x = \frac{1}{2\sqrt{2}}s(d_{\vec{r}} + d_{\vec{r}}^\dagger - u_{\vec{r}} - u_{\vec{r}^\dagger}) + \frac{1}{2\sqrt{2}}(t_{\vec{r}z}^\dagger d_{\vec{r}} + d_{\vec{r}}^\dagger t_{\vec{r}z} + t_{\vec{r}z}^\dagger u_{\vec{r}} + t_{\vec{r}z}^\dagger u_{\vec{r}})$ . In calculating  $\langle S_{1\vec{r}}^x \rangle$ , the terms including  $t_z$  or  $t_z^\dagger$  are zero since the condensed bosons  $\alpha_k$  consist of  $u(u^\dagger)$  and  $d(d^\dagger)$  only. So  $\langle S_{1\vec{r}}^x \rangle = (-1)^r m_x = \frac{1}{2\sqrt{2}}s \frac{1}{\sqrt{N}} \sum_k e^{i\vec{k}\cdot\vec{r}} \langle (d_{\vec{k}} + d_{\vec{k}}^\dagger - u_{\vec{k}} - u_{\vec{k}}^\dagger) \rangle$ . Inserting  $u_k = \chi_k \alpha_k - \rho_k \beta_k^\dagger$ ,  $d_{-k} = \chi_k \beta_k - \rho_k \alpha_k^\dagger$  and considering the condensation of  $\alpha_{\vec{k}}^\dagger$  ( $\alpha_{\vec{k}}^\dagger$ ) at  $\vec{k} = (\pi, \pi, 0)$ , we have  $\langle S_{1\vec{r}}^x \rangle = -\frac{1}{\sqrt{2}}(-1)^r \frac{s}{\sqrt{N}} (\chi_k + \rho_k) \alpha_k$  with  $k = (\pi, \pi, 0)$ . Considering  $\chi_k^2 = \frac{1}{2}(1 + \frac{A_k+B_k}{2\omega_k})$ ,  $\rho_k^2 = \frac{1}{2}(1 - \frac{A_k+B_k}{2\omega_k})$ , and  $n_h(T) = \frac{1}{N} \langle \alpha_k^\dagger \alpha_k \rangle_{\frac{A_k+B_k}{2\omega_k}}|_{k=(\pi,\pi,0)}$ , we can get  $m_x = s \sqrt{\frac{n_h(T)}{2 - d_1 - d_2}}$ .  $d_1$  and  $d_2$  are defined in equation (9).

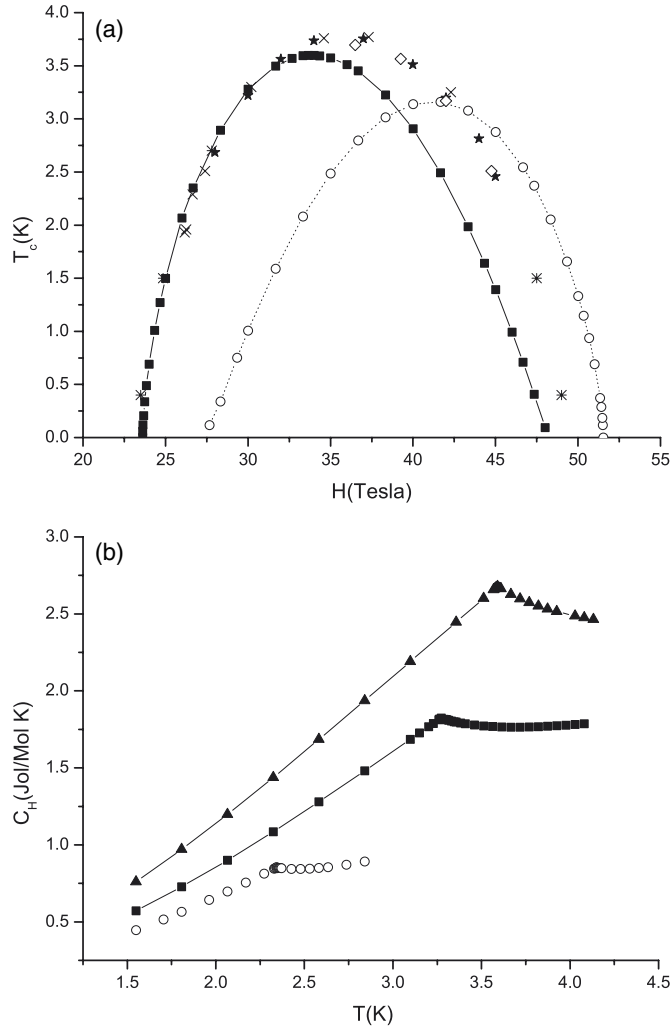


**Figure 3.** (a) Critical temperature  $T_c(h)$  with  $J = 4.45$  meV,  $J' = 0.13J$  and  $J'' = 0.026J$ . The solid line (with squares) is calculated from equations (12) (with the assumption of  $\langle s^\dagger \rangle = \langle s \rangle = s$ ) and the dotted line (with circles) from equations (19) (with the assumption of  $\langle u^\dagger \rangle = \langle u \rangle = u$ ). The experimental data for BaCuSi<sub>2</sub>O<sub>6</sub> from [5] are also plotted ( $\star$ ,  $\times$ ,  $*$ ,  $\diamond$ ). (b) Specific heat as a function of temperature for given magnetic field  $h = 0.8J$  ( $H = 26.67$  T) (circles),  $h = 0.9J$  ( $H = 30$  T) (squares) and  $h = 1.0J$  ( $H = 33.34$  T) (triangles).

of  $H$ . Remembering that  $\Delta_0 = 0.7082J$  and considering  $g = 2.306$ , we have  $H_{c1} = 23.6$  T. For small magnetic fields ( $H < 35$  T), the results agree with the experimental ones quantitatively [5], while for larger magnetic field, especially near the saturation field  $H_{c2}$ , the results deviate a little from the experimental data. Very close to  $H_{c2}$ , the critical temperature  $T_c(h)$  is difficult to obtain. The reason for this may be that  $s^2$  is too small and the assumption of  $s$  condensation is not a good starting point. We can determine the critical magnetic field  $h_{c2}$  at zero temperature from equations (12). With  $s = 0$ , we have  $m = 1$ ,  $n_h(T) = 1$  and  $\mu = -\frac{3}{4} - \frac{1}{2}(zJ' + \frac{1}{2}z'J'')$ , and then  $h_{c2} = 1 + (zJ' + \frac{1}{2}z'J'')$ . Inserting the values of  $J'$  and  $J''$ , we have  $h_{c2} = 1.546J$ . This is a little larger than the  $H_{c2} = 49$  T ( $\sim 1.48J$ ) extrapolated from the experimental data [5]. The staggered magnetization at  $H_{c2}$  is zero since  $s = 0$ .



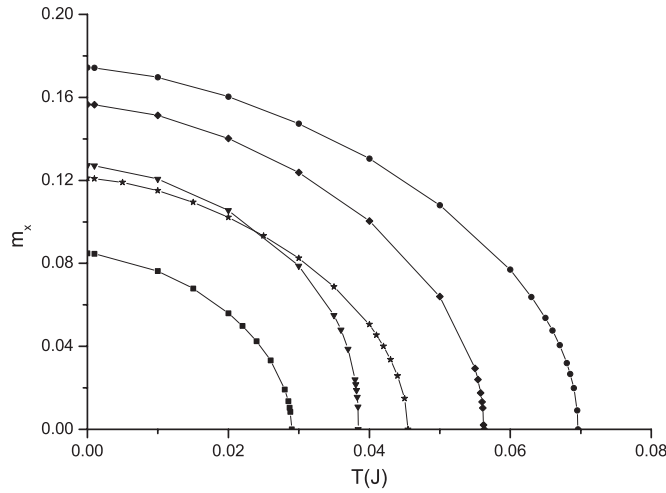


**Figure 4.** Changes in the field-induced staggered magnetization  $m_x$  with temperature in  $\text{BaCuSi}_2\text{O}_6$  with  $h = 0.75$  (squares),  $h = 0.8$  (stars),  $h = 1.0$  (circles),  $h = 1.2$  (diamonds) and  $h = 1.3$  (triangles).

In figure 3(b), we show the calculated specific heat  $C_H$  as a function of temperature at a given magnetic field  $h = 0.8\text{J}$  ( $H = 26.67\text{ T}$ ),  $h = 0.9\text{J}$  ( $H = 30\text{ T}$ ) and  $h = 1.0\text{J}$  ( $H = 33.34\text{ T}$ ), respectively. At the critical temperature  $T_c(H)$  a peak appears and the anomaly becomes sharper with increasing magnetic field ( $H < 35\text{ T}$ ). This behaviour agrees qualitatively with the experiment. At higher magnetic fields a peak can also be obtained, but the values of the specific heat is much larger than the experimental values.

Near  $h_{c1}$ , we fit the data with  $h_{c1}(T) - h_{c1}(0) \propto T^\alpha$  to determine the critical exponent  $\alpha$ . With the temperature approaching zero and the temperature window decreasing, the result converges to  $\alpha \sim 1.523$ , which agrees well with the experimentally reported value [6]. (With the revised parameters [6]  $J' = 0.51\text{ meV}$  and  $J'' = 0.168\text{ meV}$ , the fitted  $\alpha \sim 1.528$ .) The Bose–Einstein Hartree–Fock theory [16, 17], the quantum Monte Carlo simulations [14, 15] on the coupled dimer models and the self-consistent mean-field theory on an  $S = 1$  Heisenberg model with large single ion anisotropy [19] gave the same result of  $\alpha \sim 1.5$ . Experimentally, discrete values were reported in some other materials such as spin dimer systems  $\text{TlCuCl}_3$  ( $\alpha \sim 2.2$ ) and  $\text{KCuCl}_3$  ( $\alpha \sim 2.3$ ) [8]. However, the value also begins to converge to 1.5 [11].

As far as we know, there is no experimental report on the value of the field-induced staggered magnetization. In figure 4, we show the change in the field-induced staggered magnetization  $m_x$  with the external magnetic field and temperature. For a given magnetic field, the staggered magnetization decreases with increasing temperature and goes to zero at the critical temperature  $T_c(h)$ . While at a given temperature, the staggered magnetization goes up first to a maximum (occurring at  $h \sim 1.0$ , corresponding to the field with the highest  $T_c$  in figure 3(a) (solid line)) with increasing field and then decreases to zero at a certain magnetic field (depending on the given temperature, see figure 3(a)).

As discussed above, near  $H_{c2}$ , most of the dimers will be in the state of  $u^\dagger|v\rangle$ . We assume  $\langle u^\dagger \rangle = \langle u \rangle = u$  and repeat similar calculations to study the critical behaviour near  $H_{c2}$ . The details are presented in appendix B. In figure 3(a) (dotted line), we show the critical temperature  $T_c(h)$  as a function of magnetic field. This curve gives a reasonable result near  $H_{c2}$ . Fitting the data with  $h_{c2}(T) - h_{c2}(0) \propto T^{\alpha'}$ , we obtain  $\alpha' \sim 1.527$ , nearly equal to the critical exponent  $\alpha$  at  $H_{c1}$ . With  $u^2 = 1$ , we get  $h_{c2} = J + zJ' + J''$ , while with  $u^2 = 0$  we have

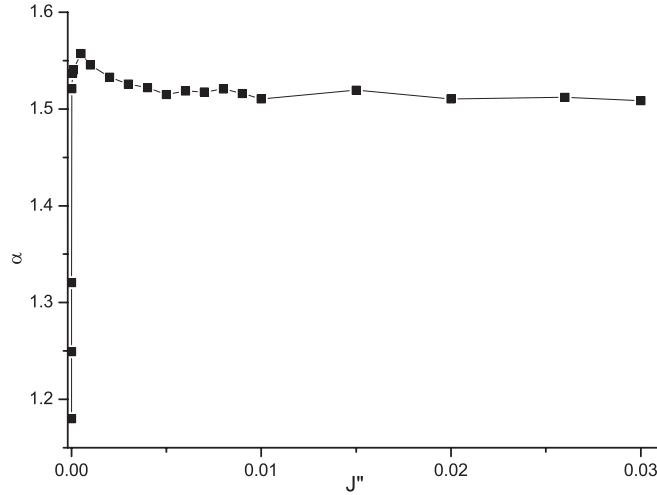


**Figure 5.** Variation of the critical exponent  $\alpha$  near  $H_{c1}$  with  $J''$  ( $J' = 0.13J$ ).

$h_{c1} = J - \frac{1}{2}zJ' - \frac{1}{2}J''$ . These two values agrees well with those obtained with the assumption of  $\langle s^\dagger \rangle = \langle s \rangle = s$ .

It was pointed out that the  $\lambda$ -shaped second-order phase transition will be replaced by a Kosterlitz–Thouless (KT) phase transition when the distance between the adjacent bilayers increases with chemical substitutions [5, 26]. Solving equations (12) and (13) with different  $J''$ , we find that  $T_c(H)$  decreases with decreasing  $J''$  and the shape of the  $T_c(H)$  curve remains similar. In figure 5, we show the variation of the critical exponent  $\alpha$  near  $H_{c1}$ .  $\alpha$  stays at about 1.5 and then drops sharply when  $J''$  approaches zero. It is interesting that a small hump can be observed just before the decrease. These behaviours may give a hint of a dimensional crossover. It should be pointed out that our solutions in the crossover region are still characteristic of a BEC, which may be an artefact of the present mean-field theory. In our calculations, the local constraint  $s^\dagger s + u^\dagger u + d^\dagger d + t_z^\dagger t_z = 1$  is replaced by a global one and the  $s(s^\dagger)$  bosons are assumed to be condensed. These approximations work well when  $s^2$  is close to 1. At higher temperatures, or in lower dimensions, thermal and/or quantum fluctuations are large and the approach does not work well. More detailed and stricter studies, especially those beyond the mean-field theory, on the crossover behaviour are expected.

## 5. Summary

In summary, we studied a quasi-two-dimensional antiferromagnet with a square-lattice bilayer structure with a bond operator formalism. The excitation shows a gap and the gap increases with increasing temperature. When the energy gap goes to zero by changing the physical parameters, a quantum phase transition from the disordered dimerized state to the Néel state occurs. When the energy gap is tuned to zero by applying an external magnetic field, some of the magnons with momentum  $(\pi, \pi, 0)$  are condensed and long range order appears in the plane perpendicular to the applied magnetic field. A phase region with field-induced long range order is obtained. The temperature and magnetic field dependences of the specific heat and the staggered magnetization are calculated. The critical exponents around  $H_{c1}$  and  $H_{c2}$  are obtained to be about 1.5. With these results, the very recent experiments on BaCuSi<sub>2</sub>O<sub>6</sub> are well interpreted. The dimensional crossover with  $J''$  approaching 0 is also discussed.

### Acknowledgments

We thank Professor Jue-Lian Shen for helpful discussions and we acknowledge financial support by the Natural Science Foundation of China.

### Appendix A. Self-consistent equations with the assumption of $\langle s^\dagger \rangle = \langle s \rangle = s$

Following equations (7),  $s^2$ ,  $\mu$  and  $m$  can be obtained by the saddle-point equations:

$$\begin{aligned}
 s^2 &= \frac{5}{2} - \frac{1}{N} \sum_k \frac{A_k + B_k}{2\omega_k} [n(\omega_k^{(1)}) + n(\omega_k^{(2)}) + 1] - \frac{1}{N} \sum_k \frac{D_k}{\Omega_k} \left[ n(\Omega_k) + \frac{1}{2} \right], \\
 \mu &= -\frac{3}{4} + \frac{1}{N} \sum_k \left[ \frac{A_k + B_k + 2C_k}{4\omega_k} [1 + n(\omega_k^{(1)}) + n(\omega_k^{(2)})] \right. \\
 &\quad \left. + \left[ n(\Omega_k) + \frac{1}{2} \right] \frac{D_k - 2F_k}{2\Omega_k} \right] \left( zJ'\gamma_k - \frac{1}{2}z'J''\gamma'_k \right), \\
 m &= \frac{1}{N} \sum_k [n(\omega_k^{(1)}) - n(\omega_k^{(2)})],
 \end{aligned} \tag{15}$$

with

$$\begin{aligned}
 \omega_k^{(1)} &= \omega_k - h + \left( \frac{1}{2}zJ' + \frac{1}{4}z'J'' \right) m \\
 \omega_k^{(2)} &= \omega_k + h - \left( \frac{1}{2}zJ' + \frac{1}{4}z'J'' \right) m \\
 \omega_k &= \sqrt{\left( \frac{A_k + B_k}{2} \right)^2 - C_k^2} \\
 \Omega_k &= \sqrt{D_k^2 - (2F_k)^2} \\
 A_k &= \frac{1}{4} - \mu - h + \left( \frac{1}{2}zJ' + \frac{1}{4}z'J'' \right) m + \frac{1}{2}zJ's^2\gamma_k - \frac{1}{4}z'J''s^2\gamma'_k \\
 B_k &= \frac{1}{4} - \mu + h - \left( \frac{1}{2}zJ' + \frac{1}{4}z'J'' \right) m + \frac{1}{2}zJ's^2\gamma_k - \frac{1}{4}z'J''s^2\gamma'_k \\
 C_k &= -\frac{1}{2}zJ's^2\gamma_k + \frac{1}{4}z'J''s^2\gamma'_k \\
 D_k &= \frac{1}{4} - \mu + \frac{1}{2}zJ's^2\gamma_k - \frac{1}{4}z'J''s^2\gamma'_k \\
 F_k &= \frac{1}{4}zJ's^2\gamma_k - \frac{1}{8}z'J''s^2\gamma'_k \\
 \gamma_k &= \frac{1}{2}(\cos k_x + \cos k_y) \\
 \gamma'_k &= \cos k_z \\
 c &= \mu N(1 - s^2) - \frac{3}{4}Ns^2 - NJ'm^2 - \frac{1}{4}NJ''m^2,
 \end{aligned} \tag{16}$$

where  $z = 4$  is the number of the nearest neighbours in a plane and  $z' = 2$  the number of the nearest neighbours in the  $z$ -direction.

### Appendix B. Self-consistent equations with the assumption of $\langle u^\dagger \rangle = \langle u \rangle = u$

Near  $H_{c2}$ , the dimer will, with most probability, be in the state of  $|\uparrow\uparrow\rangle$ . We make the assumption of  $\langle u^\dagger \rangle = \langle u \rangle = u$  and the spin operator can then be expressed as

$$\begin{aligned}
 S_{1,2}^+ &= \frac{1}{\sqrt{2}} [u(t_z \mp s) + (s^\dagger \pm t_z^\dagger)d], \\
 S_{1,2}^- &= (S_{1,2}^+)^\dagger, \\
 S_{1,2}^z &= \frac{1}{2}(u^2 - d^\dagger d \pm s^\dagger t_z \pm t_z^\dagger s).
 \end{aligned} \tag{17}$$

Inserting the above expression into Hamiltonian (1) and neglecting the three- and four-operator terms, the Hamiltonian can then be diagonalized with a Fourier–Bogliubov

transformation as

$$H = \sum_k (\Omega_{1k} a_k^\dagger a_k + \Omega_{2k} b_k^\dagger b_k + \Omega_{3k} d_k^\dagger d_k) + C_1, \quad (18)$$

with  $\Omega_{1,2k} = -\frac{1}{4}J - \mu + \frac{1}{2}J'u^2 z \gamma_k \mp \Omega_k$ ,  $\Omega_k = \sqrt{(\frac{1}{2}J + \frac{1}{4}J''z'u^2 \gamma_k')^2 + \frac{1}{4}J''^2 u^4 \sin^2 k_z}$ ,  $\Omega_{3k} = \frac{1}{4}J - \mu + h - \frac{1}{2}J'mz - \frac{1}{2}J''m$  and  $C_1 = \frac{1}{4}JNu^2 - hNu^2 + \mu N(1 - u^2) + \frac{1}{2}N(J'z + J'')(mu^2 - \frac{1}{2}m^2)$ . The self-consistent equations are then

$$\begin{aligned} u^2 &= 1 - \frac{1}{N} \sum_k [n(\Omega_{1k}) + n(\Omega_{2k}) + n(\Omega_{3k})], \\ \mu &= \frac{1}{4}J - h + \frac{1}{2}J'zm + \frac{1}{2}J''m + \frac{1}{N} \sum_k \left[ [n(\Omega_{2k}) - n(\Omega_{1k})] \frac{JJ''\gamma_k' + J''^2 u^2}{4\Omega_k} \right. \\ &\quad \left. + [n(\Omega_{2k}) + n(\Omega_{1k})] \frac{1}{2}J'z\gamma_k \right], \\ m &= u^2 - \frac{1}{N} \sum_k [n(\Omega_{3k})]. \end{aligned} \quad (19)$$

## References

- [1] Millis A J and Monien H 1993 *Phys. Rev. Lett.* **70** 2810  
 Millis A J and Monien H 1994 *Phys. Rev. B* **50** 16606
- [2] Pellegrini V, Pinczuk A, Dennis B S, Plaut A S, Pfeiffer L N and West K W 1997 *Phys. Rev. Lett.* **78** 310
- [3] Sawada A, Ezawa Z F, Ohno H, Horikoshi Y, Ohno Y, Kishimoto S, Matsukura F, Yasumoto M and Urayama A 1998 *Phys. Rev. Lett.* **80** 4534
- [4] Sasago Y, Uchinokura K, Zheludev A and Shirane G 1997 *Phys. Rev. B* **55** 8357
- [5] Jaime M, Correa V F, Harrison N, Batista C D, Kawashima N, Kazuma Y, Jorge G A, Stein R, Heinmaa I, Zvyagin S A, Sasago Y and Uchinokura K 2005 *Phys. Rev. Lett.* **93** 087203
- [6] Sebastian S E, Sharma P A, Jaime M, Harrison N, Correa V, Balicas L, Kawashima N, Batista C D and Fisher I R 2005 *Phys. Rev. B* **72** 100404
- [7] Ajiro Y, Goto T, Kikuchi H, Sakakibara T and Inami T 1989 *Phys. Rev. Lett.* **63** 1424  
 Honda Z, Katsumata K, Katori H A, Yamada K, Lhishi T, Manabe T and Yamashita M 1997 *J. Phys.: Condens. Matter* **9** L83(1997)  
 Honda Z, Asakawa H and Katsumata K 1998 *Phys. Rev. Lett.* **81** 2566
- [8] Oosawa A, Ishii H and Tanaka H 1999 *J. Phys.: Condens. Matter* **11** 265  
 Oosawa A, Aruga Katori H and Tanaka H 2001 *Phys. Rev. B* **63** 134416  
 Oosawa A, Takamasu T, Tatani K, Abe H, Tsujii N, Suzuki O, Tanaka H, Kido G and Kindo K 2002 *Phys. Rev. B* **66** 104405  
 Cavadini N, Ruegg Ch, Furrer A, Gudel H U, Kramer K, Mutka H and Vorderwisch P 2002 *Phys. Rev. B* **65** 132415  
 Ruegg C, Cavadini N, Furrer A, Gudel H U, Kramer K, Mutka H, Wildes A, Habicht K and Vorderwisch P 2003 *Nature* **423** 62
- [9] Chaboussant G, Fagot-Revurat Y, Julien M H, Hanson M E, Berthier C, Horvatic M, Levy L P and Piovesana O 1998 *Phys. Rev. Lett.* **80** 2713  
 Mayaffre H, Horvatic H, Berthier C, Julien M H, Segransan P, Levy L and Piovesana O 2000 *Phys. Rev. Lett.* **85** 4795  
 Mito M, Akama H, Kawae T, Takeda K, Deguchi H and Takagi S 2002 *Phys. Rev. B* **65** 104405
- [10] Manaka H, Yamada I, Honda Z, Katori H A and Katsumata K 1998 *J. Phys. Soc. Japan* **67** 3913  
 Hammar P R, Reich D H, Broholm C and Trouw F 1998 *Phys. Rev. B* **57** 7846  
 Stone M B, Zaliznyak I, Reich D H and Broholm C 2001 *Phys. Rev. B* **64** 144405  
 Tennant D A, Broholm C, Reich D H, Nagler S E, Granroth G E, Barnes T, Damle K, Xu G, Chen Y and Sales B C 2003 *Phys. Rev. B* **67** 054414
- [11] Paduan-Filho A, Gratens X and Oliveira N F Jr 2004 *Phys. Rev. B* **69** 020405(R)  
 Paduan-Filho A, Gratens X and Oliveira N F Jr 2004 *J. Appl. Phys.* **95** 7537

- Zapt V S, Zocco D, Hansen B R, Jaime M, Harrison N, Batista C D, Kenzelmann M, Niedermayer C, Lacerda A and Paduan-Filho A 2006 *Phys. Rev. Lett.* **96** 077204
- [12] Matsubara T and Matsuda H 1956 *Prog. Theor. Phys.* **16** 569
- [13] Affleck I 1991 *Phys. Rev. B* **43** 3215
- [14] Wessel S, Olshani M and Haas S 2001 *Phys. Rev. Lett.* **87** 206407  
Nohadani O, Wessel S, Normand B and Haas S 2004 *Phys. Rev. B* **69** 220402(R)
- [15] Kawashima N 2004 *J. Phys. Soc. Japan* **73** 3219
- [16] Nikuni T, Oshikawa M, Oosawa A and Tanaka H 2000 *Phys. Rev. Lett.* **84** 5868
- [17] Misguich G and Oshikawa M 2004 *J. Phys. Soc. Japan* **73** 3429
- [18] Matsumoto M, Normand B, Rice T M and Sigrist M 2002 *Phys. Rev. Lett.* **89** 077203
- [19] Wang H-T and Wang Y 2005 *Phys. Rev. B* **71** 104429
- [20] Hida K 1992 *J. Phys. Soc. Japan* **61** 1013
- [21] Sandvik A W and Scalapino D J 1994 *Phys. Rev. Lett.* **72** 2777
- [22] Kotov V N, Sushkov O, Zheng W and Oitmaa J 1998 *Phys. Rev. Lett.* **80** 5790  
Shevchenko P V, Sandvik A W and Sushkov O P 2000 *Phys. Rev. B* **61** 3475
- [23] Zheng W 1997 *Phys. Rev. B* **55** 12267
- [24] Matsushita Y, Gelfand M P and Ishii C 1999 *J. Phys. Soc. Japan* **68** 247
- [25] Gu Q, Yu D-K and Shen J-L 1999 *Phys. Rev. B* **60** 3009
- [26] Troyer M and Sachdev S 1998 *Phys. Rev. Lett.* **81** 5418
- [27] Sommer T, Vojta M and Becker K W 2001 *Eur. Phys. J. B* **23** 329
- [28] Sachdev S and Bhatt R N 1990 *Phys. Rev. B* **41** 9323
- [29] Wang H-T, Shen J-L and Su Z-B 1997 *Phys. Rev. B* **56** 14435
- [30] Popov V N and Fedotov S A 1988 *Sov. Phys.—JETP* **67** 535
- [31] Veits O, Oppermann R, Bindergerger M and Stein J 1994 *J. Physique I* **4** 493
- [32] Hirsch J E and Tang S 1989 *Phys. Rev. B* **39** 2850  
Sarker S, Jayaprakash C, Krishnamurthy H R and Ma M 1989 *Phys. Rev. B* **40** 5028